entropy

MDPI

Article

The Effect of Spin Squeezing on the Entanglement Entropy of Kicked Tops

Ernest Teng Siang Ong [1,†] and Lock Yue Chew [1,2,*,†]

1 Division of Physics and Applied Physics, School of Physical and Mathematical Sciences, Nanyang Technological University, 21 Nanyang Link, Singapore 637371, Singapore; on0001st@e.ntu.edu.sg
2 Complexity Institute, Nanyang Technological University, 18 Nanyang Drive, Singapore 637723, Singapore
* Correspondence: lockyue@ntu.edu.sg; Tel.: +65-6316-2968 or +65-6795-7981
† These authors contributed equally to this work.

Academic Editors: Gerardo Adesso and Jay Lawrence
Received: 20 November 2015; Accepted: 22 March 2016; Published: 2 April 2016

Abstract: In this paper, we investigate the effects of spin squeezing on two-coupled quantum kicked tops, which have been previously shown to exhibit a quantum signature of chaos in terms of entanglement dynamics. Our results show that initial spin squeezing can lead to an enhancement in both the entanglement rate and the asymptotic entanglement for kicked tops when the initial state resides in the regular islands within a mixed classical phase space. On the other hand, we found a reduction in these two quantities if we were to choose the initial state deep inside the chaotic sea. More importantly, we have uncovered that an application of periodic spin squeezing can yield the maximum attainable entanglement entropy, albeit this is achieved at a reduced entanglement rate.

Keywords: quantum entanglement; chaos; quantum squeezing

1. Introduction

The quantum kicked top is an important model for the fundamental study of quantum chaos [1–4]. It is a paradigm that is fruitful for both analytical and numerical investigations on the influence of classical chaos on various quantum features [5,6]. The manner in which chaos manifests itself in quantum mechanics has been demonstrated through the spectral properties of the generating Hamiltonian [7], hypersensitivity to perturbations [2], fidelity decay [8,9], phase space scarring [10] and entanglement [3,11–17]. Current research has found that the production rate of entanglement between two systems can be enhanced not only by increasing the coupling strength between the tops; it can also be raised by initializing the states of the quantum system within its corresponding classical chaotic phase space in the semi-classical regime [11]. In fact, entanglement is of primary interest in recent years due to its possible applications in the field of quantum information processing and its relevance to the design of quantum devices [18,19].

On the other hand, squeezing is a technique that redistributes the uncertainty within a state such that the subsequent measurements of one of a set of non-compatible observables can be enhanced and made more accurate. The idea of squeezing has been applied experimentally to improve the precision of measurement devices, for example in Ramsey spectroscopy [20], atomic clocks [21–23] and gravitational-wave detectors [24]. In addition, squeezing has also been employed for the purpose of detecting quantum entanglement [25,26]. All of these applications of squeezing have pointed to its important role in advancing the development of technologies and systems based on the theory of quantum mechanics.

The close relationship between squeezing and quantum entanglement brings up the question of how the active application of spin squeezing can affect the entanglement of two coupled quantum kicked tops. To answer this question, we have built upon the model and results of Miller and

Sakar [12], who have demonstrated that the rate of entanglement increase for the coupled kicked tops is intrinsically dependent on its classical chaotic dynamics. Our contribution in this paper is the inclusion of an additional spin squeezing procedure by Kitagawa and Ueda [27] to our model, where we either squeeze the spin initially before time evolution or squeeze the spin periodically. Our results show the efficacy of using spin squeezing to boost the generation of entanglement entropy, especially by means of periodic squeezing.

Our paper is organized as follow. In Section 2, we provide the technical details of the two-coupled quantum kicked tops with regards to their initial state, time evolution and the spin squeezing procedure. In Section 3, we discuss the corresponding classical dynamics and phase space of the quantum kicked tops, as well as the semi-classical representation based on the Husimi Q function. In Section 4, we give the mathematical preliminaries and definitions that are required for a quantitative definition of quantum entanglement, and in Section 5, we proceed to present and discuss our numerical results. Finally, Section 6 concludes the paper.

2. Two-Coupled Quantum Kicked Tops

2.1. Kicked Tops

The kicked top is a simple dynamical system characterized by the state of its angular momentum. It is an excellent model for the theoretical and experimental study on quantum chaos in lieu of its association with a finite-dimensional quantum Hilbert space and a corresponding classical phase space that is low-dimensional [2,3,28]. The Hamiltonian of a quantum kicked top takes the form:

$$\hat{H}(t) = \frac{\pi}{2\tau}\hat{J}_y + \frac{k}{2j}\hat{J}_z^2 \sum_{n=-\infty}^{\infty} \delta(t - n\tau) \tag{1}$$

with the first term representing the precession of the top at an angular frequency of $\pi/2$ about the y-axis. The second term indicates that the top is being kicked regularly at a fixed period τ, leading to an impulsive rotation about the z-axis, which is proportional to the dimensionless factor k/j. Specifically, k is the strength of the kick, while j is simply the quantum number of the system. By working in discrete time and setting τ to one, the time evolution of the kicked top can be determined through the following unitary operator:

$$\hat{U}' = \hat{U}_k'\hat{U}_f' = \exp(-\frac{ik}{2j}\hat{J}_z^2)\exp(-i\frac{\pi}{2}\hat{J}_y) \tag{2}$$

In this paper, our principal interest is on coupled kicked top systems. In particular, we are interested in the effects of squeezing the initial states of the kicked tops on their entanglement dynamics. For this investigation, we require the Hamiltonian of a two-coupled quantum kicked top system, which involves a sum of the Hamiltonian of each kicked top plus an additional term on the spin-spin interaction:

$$\begin{aligned}\hat{H}(t) = \frac{\pi}{2\tau}\hat{J}_{y_1} + \frac{k}{2j}\hat{J}_{z_1}^2 \sum_{n=-\infty}^{\infty} \delta\left(t - n\tau\right) + \frac{\pi}{2\tau}\hat{J}_{y_2} \\ + \frac{k}{2j}\hat{J}_{z_2}^2 \sum_{n=-\infty}^{\infty} \delta\left(t - n\tau\right) + \frac{k\varepsilon}{j}\hat{J}_{z_1}\hat{J}_{z_2} \sum_{n=-\infty}^{\infty} \delta\left(t - n\tau\right)\end{aligned} \tag{3}$$

Note that the strength of the interaction is proportional to the dimensionless constant $k\varepsilon/j$, with ε being the coupling constant between the two tops. With this formulation, the unitary time evolution is then given by:

$$\hat{U} = \hat{U}_{\varepsilon_{12}}\hat{U}_{c_1}\hat{U}_{c_2} = \hat{U}_{k_1}\hat{U}_{k_1}\hat{U}_{\varepsilon_{12}}\hat{U}_{f_1}\hat{U}_{f_2} \tag{4}$$

and the details of the various terms are stated below:

$$\hat{U}_{c_r} := \hat{U}_{k_r} \hat{U}_{f_r} \tag{5}$$

$$\hat{U}_{f_r} := \exp\left(-\frac{i\pi}{2} \hat{J}_{y_r}\right) \tag{6}$$

$$\hat{U}_{k_r} := \exp\left(-\frac{ik}{2j} \hat{J}_{z_r}^2\right) \tag{7}$$

$$\hat{U}_{\varepsilon_{12}} = \exp\left(-\frac{ik\varepsilon}{j} \hat{J}_{z_1} \hat{J}_{z_2}\right) \tag{8}$$

Note that the index r is to be taken as either one or two from now on.

2.2. Initial States

Coherent states are the most "classical" states, and they are thus directly relevant to our investigation of quantum-classical correspondence. In particular, the directed angular momentum states $|\theta_0, \phi_0\rangle$ [2,28,29] are the coherent states of the quantum kicked top system. Such states are also widely known as the atomic coherent states, and they are of main interest as initial quantum states in this paper. They can be simply generated by applying a rotation operator on the eigenstate $|j, j\rangle$:

$$|\theta_0, \phi_0\rangle = \exp\left[i\theta_0 \left(\hat{J}_x \sin\phi_0 - \hat{J}_y \cos\phi_0\right)\right] |j, j\rangle \tag{9}$$

The result can be further expressed in terms of the $|j, m\rangle$ basis after performing Taylor expansion, and it is found that [30]:

$$|\theta_0, \phi_0\rangle = (1 + \gamma\gamma^*)^{-j} \sum_{m=-j}^{j} \gamma^{j-m} \sqrt{\binom{2j}{j+m}} |j, m\rangle \tag{10}$$

where:

$$\gamma = \exp(i\phi_0) \tan\left(\frac{\theta_0}{2}\right) \tag{11}$$

By taking a direct product of these individual kicked top states, we obtain the initial states of our two-coupled kicked top system:

$$|\psi(0)\rangle = |\theta_{0_1}, \phi_{0_1}\rangle \otimes |\theta_{0_2}, \phi_{0_2}\rangle \tag{12}$$

2.3. Quantum Kicked Top Evolution

To initialize the state of our quantum kicked tops, Equation (10) is first used to generate the initial state of each of the two separate kicked top. The initial state of the entire system is then obtained through a tensor product of these individual states according to Equation (12). The quantum state of the kicked top at a future time step is then determined by the unitary time evolution operator given by Equation (4) acting on the quantum state at a previous time step starting with the initial state. This allows the kicked top to evolve at a discrete time step of $n\tau$ (for $n = 0, 1, 2, \ldots$). In the Schrödinger picture, the time evolution of the quantum state of the kicked tops at time step n then takes the following form:

$$\begin{aligned} &\langle s_1, s_2 | \psi(n) \rangle \\ &= \langle s_1, s_2 | U | \psi(n-1) \rangle \qquad (13) \\ &= \sum_{s_1'=-j}^{+j} \sum_{s_2'=-j}^{+j} \langle s_1, s_2 | U_{\varepsilon_{12}} | s_1', s_2' \rangle \langle s_1', s_2' | U_{c_1} U_{c_2} | \psi(n-1) \rangle \qquad (14) \end{aligned}$$

where $|s_1', s_2'\rangle$ and $|s_1, s_2\rangle$ are arbitrary states. Note that we have dropped j_1 and j_2 from the notation $|j_1, m_1, j_2, m_2\rangle$, since they are fixed at 80. The term $\langle s_1, s_2| U_{\varepsilon_{12}} |s_1', s_2'\rangle$ can be easily simplified using the fact that the initial states are in the J_z basis, *i.e.*,

$$\hat{J}_z |m\rangle = m |m\rangle \tag{15}$$

This leads to:

$$\begin{aligned} &\langle s_1, s_2|\psi(n)\rangle \\ &= \sum_{s_1'=-j}^{+j} \sum_{s_2'=-j}^{+j} \exp\left(-\frac{ik\varepsilon}{j} s_1' s_2'\right) \langle s_1, s_2|s_1', s_2'\rangle \langle s_1', s_2'| U_{c_1} U_{c_2} |\psi(n-1)\rangle \\ &= \exp\left(-\frac{ik\varepsilon}{j} s_1 s_2\right) \langle s_1, s_2| U_{c_1} U_{c_2} |\psi(n-1)\rangle \end{aligned} \tag{16}$$

The last term of Equation (16) can be evaluated as follows:

$$\begin{aligned} &\langle s_1, s_2| U_{c_1} U_{c_2} |\psi(n-1)\rangle \\ &= \sum_{m_1=-j}^{+j} \sum_{m_2=-j}^{+j} \langle s_1| U_{c_1} |m_1\rangle \langle s_2| U_{c_2} |m_2\rangle \langle m_1, m_2|\psi(n-1)\rangle \end{aligned} \tag{17}$$

Both $\langle s_1| U_{c_1} |m_1\rangle$ and $\langle s_2| U_{c_1} |m_2\rangle$ are then determined using Equation (5):

$$\langle s_r| U_{c_r} |m_r\rangle = \langle s_r| U_{k_r} U_{f_r} |m_r\rangle \tag{18}$$

$$= \exp\left(-\frac{ik}{2j} s_r^2\right) \langle s_r| U_{f_r} |m_r\rangle \tag{19}$$

Using the fact that U_{f_r} is a rotational unitary group operator, we are able to evaluate and obtain the following result [31,32]:

$$\langle s_r| U_{f_r} |m_r\rangle = \frac{(-1)^{s_r - m_r}}{2^j} \binom{2j}{j - s_r}^{1/2} \binom{2j}{j + m_r}^{-1/2} \tag{20}$$

$$\times \sum_{\nu} (-1)^{\nu} \binom{j - s_r}{\nu} \binom{j + s_r}{\nu + s_r - m_r} \tag{21}$$

This expression can also be expressed in the following alternative form by expanding upon the binomial coefficient:

$$\langle s_r| U_{f_r} |m_r\rangle = \frac{(-1)^{s_r - m_r}}{2^j} \sum_{\nu} (-1)^{\nu} \frac{\sqrt{(j - s_r)!(j + s_r)!(j + m_r)!(j - m_r)!}}{\nu!(j - s_r - \nu)!(j + m_r - \nu)!(\nu + s_r - m_r)!} \tag{22}$$

Note that the summation across ν is performed for all values of ν, such that the denominator of Equation (22) is finite. Furthermore, the factorial of a negative integer is taken to be infinite based on the relation between the factorial and the gamma function.

2.4. Spin Squeezing

Quantum squeezing has the effect of reducing the uncertainty in an observable while increasing the uncertainty of its non-commuting counterpart. For our quantum kicked tops system, we apply squeezing to the coherent angular momentum or spin states of the tops either at the initial instant or

at a periodic interval. Our system is considered squeezed when the variance of one of its observables satisfies the following inequality [33]:

$$\left(\Delta \hat{J}_i^2\right) \leq \left|\langle \hat{J}_k \rangle\right| / 2 \tag{23}$$

in relation to the quantum uncertainty product:

$$\left(\Delta \hat{J}_i^2\right)\left(\Delta \hat{J}_j^2\right) \geq \left|\langle \hat{J}_k \rangle\right|^2 / 4 \tag{24}$$

with i, j and k being components in any three orthogonal directions. This perspective is in line with the definition of spin squeezing proposed by Kitagawa and Ueda [27]. In their paper, they proposed that it is possible to minimize fluctuations in one spin direction at the expense of enhancing the fluctuations in the other directions. In other words, a spin is considered squeezed only if the variance of a spin component normal to the mean spin vector is less than the standard quantum limit, which has been shown by Kitagawa and Ueda to be $S/2$ for a system with S spin.

In order for squeezing to occur, a nonlinear interaction is needed as a linear interaction simply rotates the spin vectors and does not establish quantum correlations among them. This leads us to employ a class of unitary operators with a nonlinear Hamiltonian for our squeezing operation:

$$\hat{H} = \hbar F\left(\hat{J}_z\right) \tag{25}$$

where $F\left(\hat{J}_z\right)$ is a nonlinear function of the z-axis angular momentum operator, and thus:

$$\hat{U}_s\left(\beta\right) = \exp\left[-i\beta F\left(\hat{J}_z\right)\right] \tag{26}$$

If we were to consider the lowest-order nonlinear interaction term for the Hamiltonian:

$$F\left(\hat{J}_z\right) = \chi \hat{J}_z^2 \tag{27}$$

with χ being a constant of proportionality, we obtain an interaction that causes a twist in the quantum fluctuations and is analogous to self-phase modulation in a photonic system. This gives rise to the one-axis twisting squeeze operator:

$$\hat{U}_s\left(\mu\right) = \exp\left(-i\mu \hat{J}_z^2/2\right) \tag{28}$$

with the factor:

$$\mu \equiv 2\chi\beta \tag{29}$$

quantifying the degree and strength of squeezing of the squeeze operator. By adjusting μ, we create spin squeezed states as follows:

$$\begin{aligned} \left|\theta_{0_1}, \phi_{0_1}\right\rangle_s \otimes \left|\theta_{0_2}, \phi_{0_2}\right\rangle_s &= \left(\hat{U}_{s_1}\left(\mu\right) \otimes \hat{U}_{s_2}\left(\mu\right)\right)\left|\psi\left(0\right)\right\rangle \\ &= \exp\left(-i\mu \hat{J}_{z_1}^2/2\right)\left|\theta_{0_1}, \phi_{0_1}\right\rangle \otimes \exp\left(-i\mu \hat{J}_{z_2}^2/2\right)\left|\theta_{0_2}, \phi_{0_2}\right\rangle \end{aligned} \tag{30}$$

and:

$$\begin{aligned} \left|\theta_{(n\tau)_1}, \phi_{(n\tau)_1}\right\rangle_s \otimes \left|\theta_{(n\tau)_2}, \phi_{(n\tau)_2}\right\rangle_s &= \left(\hat{U}_{s_1}\left(\mu\right) \otimes \hat{U}_{s_2}\left(\mu\right)\right)\left|\psi\left(n\tau\right)\right\rangle \\ &= \exp\left(-i\mu \hat{J}_{z_1}^2/2\right)\left|\theta_{(n\tau)_1}, \phi_{(n\tau)_1}\right\rangle \\ &\quad \otimes \exp\left(-i\mu \hat{J}_{z_2}^2/2\right)\left|\theta_{(n\tau)_2}, \phi_{(n\tau)_2}\right\rangle \end{aligned} \tag{31}$$

Note that the former spin squeezed state results from initial spin squeezing, while the latter periodic spin squeezing with period τ at $n = 0, 1, 2, \ldots$, where squeezing has been performed at the same factor μ for both tops. In addition, since our directed angular momentum states are expressed in terms of the J_z basis, the application of $U_s(\mu)$ on state $|m\rangle$ for a top is equivalent to the same state being acted upon by:

$$\hat{U}_s = \exp\left(-i\mu m^2/2\right) \tag{32}$$

This simplifies the computation of the squeezing operator, as well as the consequential tensor product state.

Let us illustrate the effect of μ on spin state squeezing for a single top on a quasiprobability distribution based on the Husimi Q function plotted using the QuTiP toolbox (Version 3.1.0) [34,35]. First, an unsqueezed kicked top possesses a state with quantum fluctuations that follow a Gaussian distribution. In this case, the cross-section of the quasiprobability distribution is circular with a high probability in the center that reduces as it goes outwards, as shown in Figure 1. By using this spin coherent state with the squeezing operator given by Equation (28) at $\mu = 0.2$, we obtain a squeezed state which is stretched in both the x- and y-directions, as shown in Figure 2. It is important to note that too large a μ is inappropriate, as the resulting spin squeezed state can be broken up, as shown in Figure 3 for $\mu = 10$. In this paper, we have fixed $\mu = 0.2$, as the resulting state is substantially squeezed to sample a wider range of the quantum states in the Hilbert space without the state being broken up.

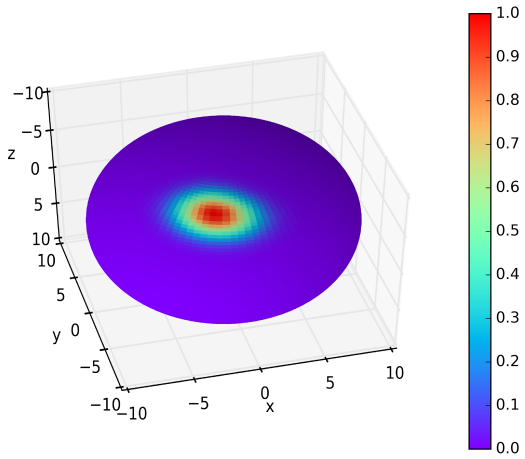

Figure 1. The quasiprobability density of the coherent state based on the spin Q function is shown here mapped onto a sphere, which is its phase space. The state follows a Gaussian distribution, and the area of the plot indicates the uncertainty of the state. Note that $j = 80$.

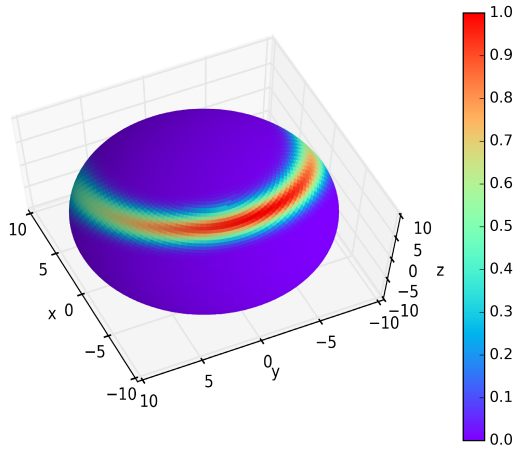

Figure 2. The quasiprobability density of the spin squeezed state after the coherent state has been acted on by the one-axis twisting squeeze operator with $\mu = 0.2$. Note that the resulting state is elongated and stretched in both the x- and y-direction. Note that $j = 80$.

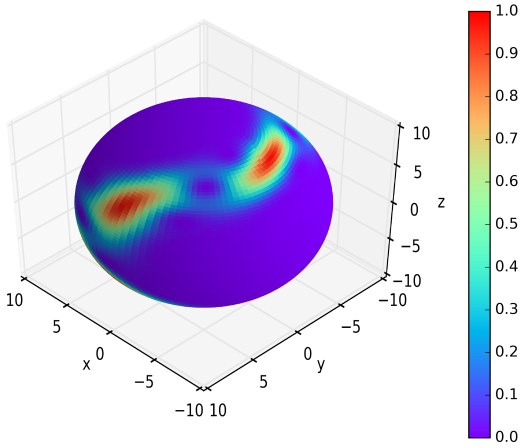

Figure 3. The quasiprobability density of the state after the action of the one-axis twisting squeeze operator on the coherent state at $\mu = 10$. The state has split into multiple islands, which is not suitable for our study of quantum-classical correspondence, since the integrity of a squeezed state has been destroyed. Note that $j = 80$.

Mathematically, the spin Q function is defined as:

$$Q(\theta, \phi) = \frac{1}{\pi} \langle \alpha | \hat{\rho} | \alpha \rangle \tag{33}$$

where $\hat{\rho}$ is the density matrix of the system:

$$\hat{\rho} = |\psi(0)\rangle \langle \psi(0)| \tag{34}$$

and α is given by:

$$\begin{aligned} \alpha &= x + iy \\ &= \sin\theta \cos\phi + i \sin\theta \sin\phi \end{aligned} \tag{35}$$

3. Quantum-Classical Correspondence

It is possible to rescale the angular momentum variables and, through the Heisenberg equations obtained, a set of classical equations of the two-coupled kicked tops in terms of c-number variables. Nonetheless, in analogy to the approach of Miller and Sarkar, we shall consider a single decoupled classical kicked top instead and exploit its phase space for our theoretical analysis on the problem of the quantum-classical correspondence of the two-coupled quantum kicked tops with spin squeezing. In this context, by first defining the classical variables:

$$\vec{V} = (X, Y, Z) := \frac{\vec{J}}{j} \left(\hat{J}_x, \hat{J}_y, \hat{J}_z \right) \tag{36}$$

and setting the angle of precession about the y-axis to $\pi/2$, the following recursion relation for a single kicked top has been obtained:

$$\begin{aligned} X' &= Z\cos(kX) + Y\sin(kX) \\ Y' &= -Z\cos(kX) + Y\sin(kX) \\ Z' &= -X \end{aligned} \tag{37}$$

at the classical limit, as well as negligible coupling between the two tops. By re-expressing these variables in terms of [29]:

$$\begin{aligned} \theta &= \arccos Z \\ \phi &= \arctan \frac{Y}{X} \end{aligned} \tag{38}$$

which lie on the surface of a unit sphere, we can make a direct correspondence between the classical and the quantum states. In terms of θ and ϕ, which corresponds to the direct angular momentum state, we have plotted the phase space map of the kicked top using Equations (37) and (38) with an iteration of over 10^5 kicks (see Figure 4). This classical phase portrait shows the stroboscopic time evolution of the kicked top with the period of the kicks being matched to the discrete time evolution of the top. In this paper, we have fixed the parameter k to three. In this regime, the classical dynamics of the kicked top exhibits a mixture of regular and chaotic dynamics. This is evident through the presence of both regular islands and a chaotic sea in Figure 4. We have chosen six different initial conditions to sample different regions of the phase space for our simulation. Specifically, we have selected two points within the regular island and four points at various positions in the chaotic region. Two of the points, ($\phi = 0.63$, $\theta = 2.10$) and ($\phi = 0.63$, $\theta = 2.00$), are chosen, such that they are close to the edge that separates regions of chaos and regularity.

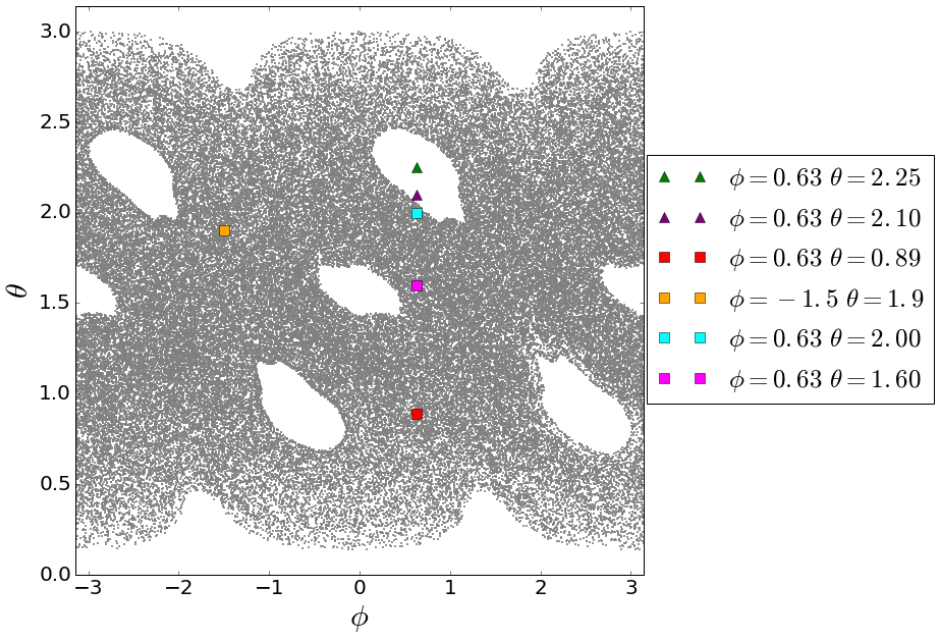

Figure 4. Phase space map for $k = 3$ with six initial conditions marked in the plot. Note that the triangle markers represent the coordinates of the regular kicked tops, while the square markers represent the coordinates of the chaotic kicked top.

4. Quantification of Entanglement

There are various ways to quantify entanglement, such as the use of Bell's inequalities and concurrence [36]. Since our states of consideration are pure states, we shall employ the von Neumann entropy of the subsystem state as our measure of entanglement. For this calculation, we first obtain the time-evolved state of the two-coupled quantum kicked top $|\psi(n)\rangle$ at time step n, from which we yield the density matrix ρ of the system as follows:

$$\rho(n) = |\psi(n)\rangle \langle\psi(n)| \tag{39}$$

We then determine the reduced density matrix by taking a partial trace of the density matrix over one of the subsystem. For example, in order to obtain the reduced density matrix of the first kicked top, we perform a partial trace over the density matrix with respect to the second kicked top:

$$\rho_1(n) = \mathrm{Tr}_2[\rho(n)] \tag{40}$$

Alternatively, the reduced density matrix can also be obtained directly from the state of the system. In this case, the reduced density matrix can be represented in the matrix form as follows:

$$\langle m_1|\rho_1|n_1\rangle = \sum_{n_2=-j}^{+j} \langle m_1, n_2|\psi(n)\rangle \langle\psi(n)|n_1, n_2\rangle \tag{41}$$

The entanglement entropy of the system is then calculated from the von Neumann entropy of the reduced density matrix of the first kicked top in the following manner:

$$E(n) := -\mathrm{Tr}_1[\rho_1(n) \ln \rho_1(n)] \tag{42}$$

This calculation can be simplified by first diagonalizing the reduced density matrix $\rho_1(n)$ to obtain the set of $2j+1$ eigenvalues $\lambda_i(n)$. This leads to the following entanglement entropy of the two-coupled kicked tops at time step n:

$$E\left(n\right) = -\sum_{i=-j}^{+j} \lambda_i(n) \ln \lambda_i(n) \tag{43}$$

5. Results and Discussion

5.1. Entanglement without Spin Squeezing

We first investigate the entanglement dynamics of the two-coupled quantum kicked tops without spin squeezing. Note that we have adopted a value of $\varepsilon = 0.001/3$ for the coupling coefficient of the tops, since this value gives a reasonable rate of entanglement increase between the tops in our simulation studies. We have also set the coupled kicked tops at the parameter value $k = 3$. For the time-evolution of the kicked tops, we first consider three types of initial states: (i) the regular-regular $|\theta_r, \phi_r\rangle \otimes |\theta_r, \phi_r\rangle$; (ii) the regular-chaotic $|\theta_r, \phi_r\rangle \otimes |\theta_c, \phi_c\rangle$; and (iii) the chaotic-chaotic $|\theta_c, \phi_c\rangle \otimes |\theta_c, \phi_c\rangle$, where $(\theta_r, \phi_r) = (2.25, 0.63)$ and $(\theta_c, \phi_c) = (0.89, 0.63)$. From our simulations, we observe that the entanglement increases at a linear rate, but the entanglement rate of the $|\theta_c, \phi_c\rangle \otimes |\theta_c, \phi_c\rangle$ initial state is much greater than the other two cases when at least one of the tops is regular (see Figure 5). This result shows that starting with initial quantum states, which correspond to chaotic states of the kicked tops in the classical regime, has the propensity of enhancing the entanglement dynamics in the quantum regime.

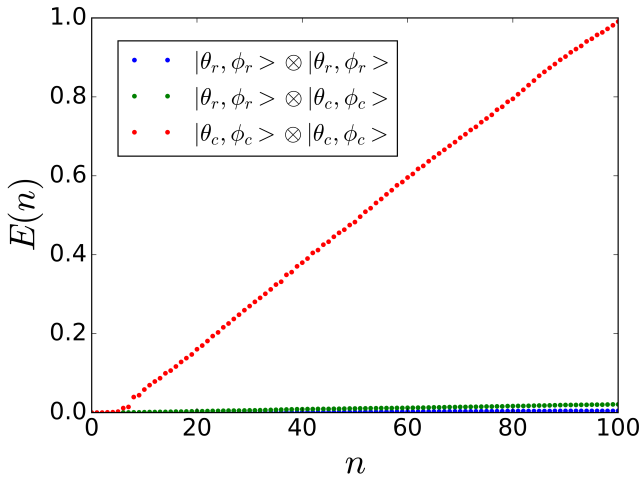

Figure 5. A plot of the entanglement dynamics of the kicked tops evolution without spin squeezing. The entanglement rate for the kicked tops with a regular-regular initial state is extremely low over the 100 time steps. The case where at least one of the tops is chaotic has a slight increase in entanglement rate, while the entanglement rate is highest for the chaotic-chaotic initial state.

Our results agree with that by Miller and Sarkar [12]. In their paper, they have shown a linear rate of increase of entanglement. By computing beyond $n = 100$, we have further observed a saturation of the von Neumann entropy. The asymptotic von Neumann entropy is expected to fall below the statistical bound of $\ln\left(e^{-1/2}\mathcal{N}\right)$, where $\mathcal{N}$ is the dimension of the Hilbert space [37]. As the spin Hilbert space is of dimension 161 for $j = 80$, this gives a maximum theoretical value of 4.58 for the entanglement of the system, which is close to our observed value of four (see Figure 6).

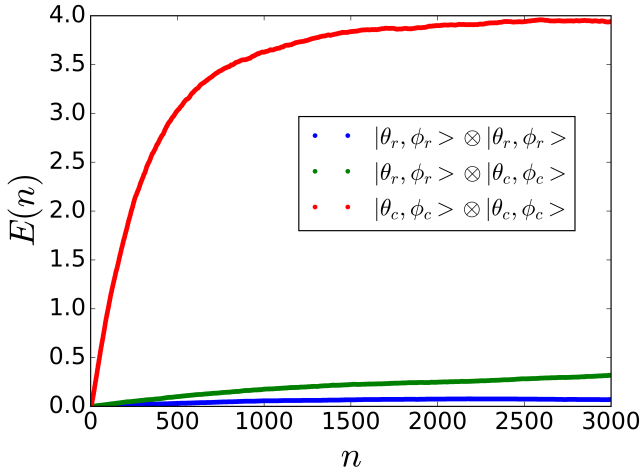

Figure 6. A plot of the entanglement dynamics of the kicked tops for a total of 3×10^3 time steps. The entanglement rates are linear initially, but approach saturation subsequently. Our simulation results show that only the kicked tops starting with the chaotic-chaotic initial state are near to the maximum statistical bound of 4.58 for the entanglement entropy.

A qualitative explanation of the connection between entanglement enhancement and the dynamical behavior of the corresponding initial classical states can be understood as follows. While the kicked tops are initialized in a quantum state, our consideration of high j puts the system in a semi-classical regime, such that a classical analogue of the initial state becomes relevant. From this viewpoint of the classical analogue, we can perceive the states to be initialized within $\delta\theta$ and $\delta\phi$ of (θ_0, ϕ_0). For a top with regular dynamics, the trajectories are periodic or quasi-periodic. This implies that the two tops are evolving with rather similar dynamics without being easily distinguishable, and according to the notion of quantum relative entropy, the distinguishability of the dynamics is related to the entanglement between the two tops. A less distinguishable dynamics implies a lower level of entanglement entropy, which happens in the regular case. On the other hand, when the motion of the two tops are chaotic, any small variations in the kicked tops would result in a large difference in their trajectories over time. Thus, the dynamics of the two tops become more and more differentiated with time, and based on quantum relative entropy, a faster rate of initial increase with a higher level of entanglement entropy eventually attained at the long time limit is to be expected.

5.2. Initial Spin Squeezing and Periodic Spin Squeezing

Let us now squeeze the directed angular momentum coherent state either initially or periodically to observe its effect on the resulting entanglement dynamics of the two-coupled kicked tops. For this, we shall only concern ourselves with the case where the squeezing operator acts on either the regular-regular or the chaotic-chaotic initial states, as the entanglement dynamics from the regular-chaotic state is expected to be intermediate between these two extremes.

By first squeezing the initial state according to Equation (30) for the regular-regular state, we observe a substantial enhancement of the entanglement dynamics of the kicked tops against that when there is no initial spin squeezing (see Figure 7). In fact, the linear increase of the entanglement entropy here seems to correspond to that of the chaotic-chaotic initial state without spin squeezing. On the other hand, no drastic changes happen for the entanglement dynamics after the chaotic-chaotic initial state is squeezed based on Equation (30), as illustrated in Figure 8. Instead, we observe a slight decrease in the entanglement entropy in comparison to the case when no initial spin squeezing is performed on the chaotic-chaotic state. Moreover, the result here actually corresponds to the initial spin squeezed regular-regular case. We have performed further simulation runs for the spin squeezed chaotic-chaotic initial state for a total of 3×10^3 time steps to study the eventual trend

of the entanglement dynamics (see Figure 9). The results clearly show a reduced entanglement entropy compared to that when the chaotic-chaotic initial state is not spin squeezed. A qualitative explanation of these observations is as follows. Through spin squeezing, we have stretched and elongated the initial state, as illustrated in Figure 2. Since we are in the semi-classical regime, there is good quantum-classical correspondence between the quantum and classical states. From this context, a stretching of the quantum states corresponds to a stretching of the classical states. This argument implies that a stretched classical regular initial state would sample the chaotic part of the classical phase space in addition to the regular part, and by linking back to the quantum phase space through the correspondence principle, we can now envisage an enhancement in entanglement entropy as observed in our computation, since there are now chaotic elements in the initial state. Conversely, we understand why there is a drop in entanglement entropy for the initial spin squeezed chaotic state because of the additional sampling of regular initial states due to the stretching.

A study carried out by Song *et al.* [38] has shown that the squeezing effects of spin squeezed states decay over time. Furthermore, they have found that the spin squeezing effects decay faster when the dynamics of the quantum kicked top correspond to the classical chaotic regime *versus* the regular regime. This observation has led us to the idea of squeezing the time-evolved quantum state periodically according to Equation (31). Interestingly, we notice that with periodic squeezing, the entanglement rate is lower than when the quantum kicked-top has its initial state squeezed or non-squeezed. However, squeezing periodically gives rise to an eventual asymptotic entanglement entropy that is higher than the other two cases (see Figure 10). This can be understood qualitatively as before based on quantum-classical correspondence. Periodic squeezing causes the state to elongate and overlap a larger range of stable islands during the initial phase, whose consequence is a lower rate of entanglement of the quantum kicked top relative to the two cases. Subsequently, the continuous stretching of the quantum state due to periodic squeezing samples the chaotic sea increasingly, which explains the observation of higher entanglement entropy asymptotically. In fact, the above results are consistent and continue to apply when the initial states indicated in Figure 4 are employed. As illustrated in Figure 10, periodic squeezing is again observed to drive the state towards a maximum asymptotic entanglement entropy better than the case with initial squeezing or no squeezing.

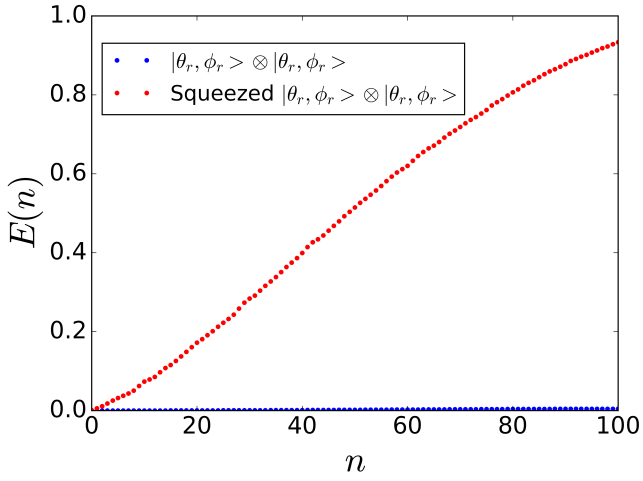

Figure 7. A comparison between the entanglement dynamics of quantum kicked tops for the case of the non-squeezed and spin-squeezed initial regular-regular state with $\mu = 0.2$. The effect of spin squeezing on the state leads to a substantial increase in entanglement that is comparable to the chaotic quantum kicked top without spin squeezing.

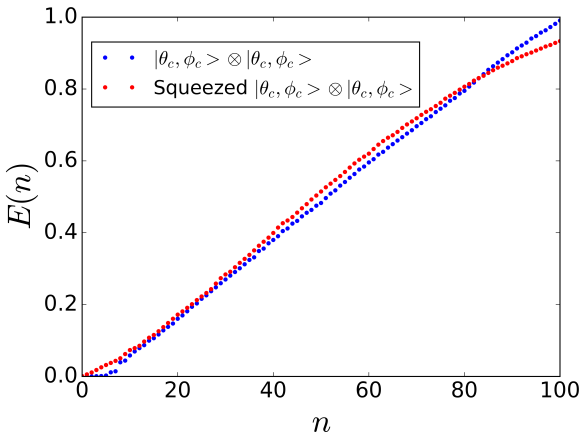

Figure 8. A comparison between the entanglement dynamics of quantum kicked tops for the case of the non-squeezed and spin-squeezed initial chaotic-chaotic state with $\mu = 0.2$. While the kicked tops with initial spin squeezing is observed to entangle at a faster rate in the beginning, its entanglement eventually drops below the case without spin squeezing.

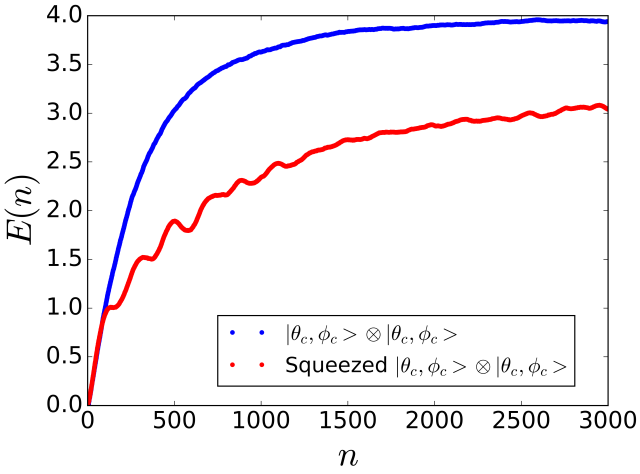

Figure 9. The entanglement dynamics of Figure 8 is extended to a total of 3×10^3 time steps. The asymptotic entanglement entropy of the kicked tops is observed to be lower for the initial spin-squeezed case compared to the case of no squeezing. The squeezing parameter is taken to be $\mu = 0.2$, and the initial states $\phi = 0.63$ and $\theta = 0.89$.

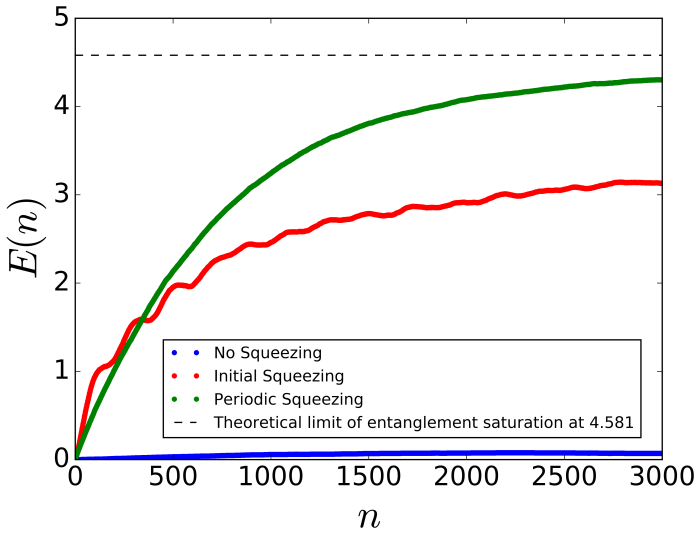

(**a**)

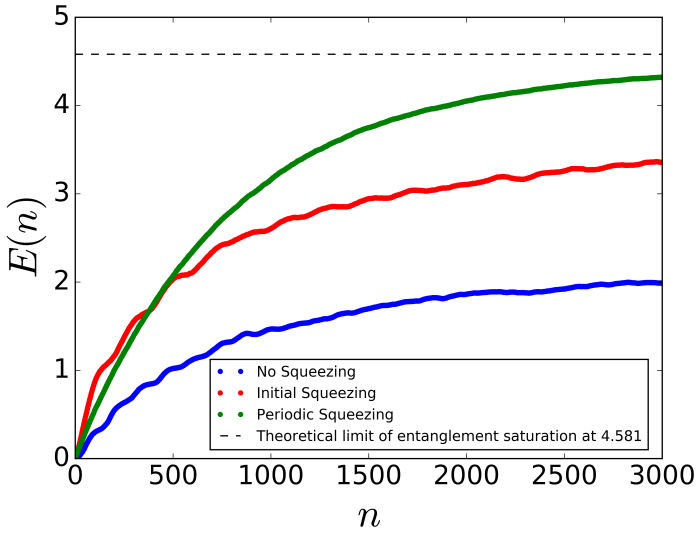

(**b**)

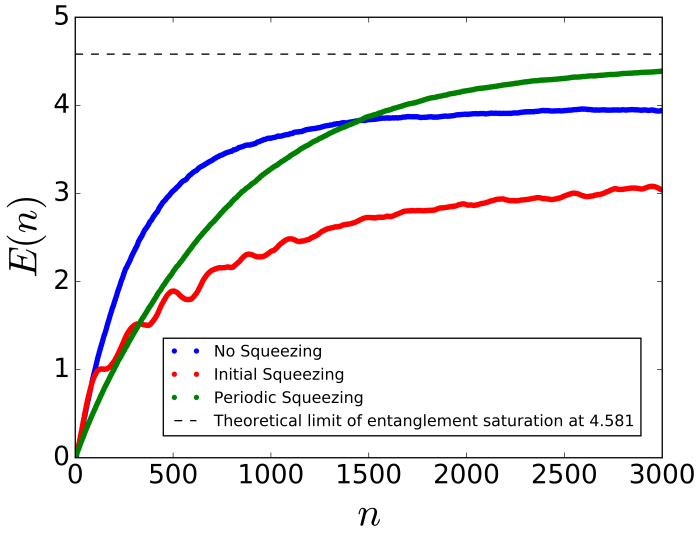

(**c**)

Figure 10. *Cont.*

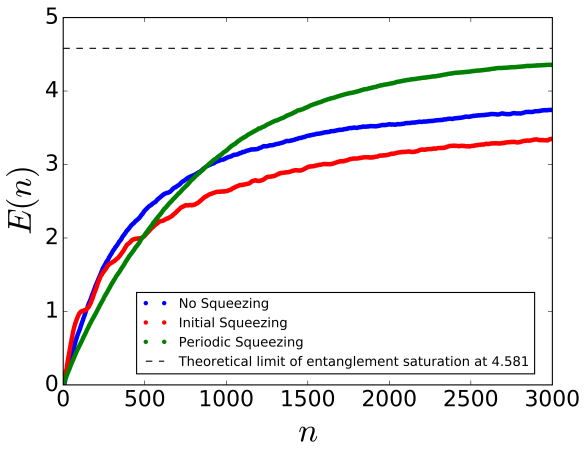

(**d**)

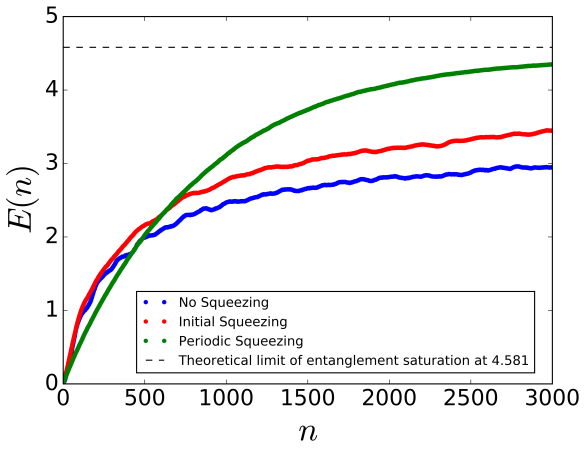

(**e**)

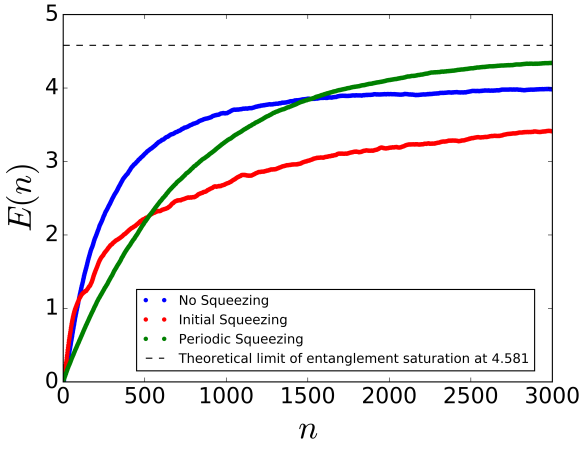

(**f**)

Figure 10. A comparison of the entanglement dynamics for the six different initial conditions indicated in the phase space map of Figure 4. The squeezing parameter is set to be $\mu = 0.2$. The dynamical behavior for the entanglement dynamics with no squeezing, with periodic spin squeezing and with initial spin squeezing is consistent with respect to the various regions of the phase space map. In particular, periodic squeezing is again shown to be most effective in generating entanglement for the various initial conditions. Note that the blue line represents no squeezing, the red line initial squeezing and the green line periodic squeezing. (**a**) $\phi = 0.63$, $\theta = 2.25$; (**b**) $\phi = 0.63$, $\theta = 2.10$; (**c**) $\phi = 0.63$, $\theta = 0.89$; (**d**) $\phi = -1.50$, $\theta = 1.90$; (**e**) $\phi = 0.63$, $\theta = 2.00$; (**f**) $\phi = 0.63$, $\theta = 1.60$.

The above argument can be further supported by the consideration of quantum kicked-tops that operate in a full chaotic phase space. According to our previous qualitative analysis, we would expect the three cases of no squeezing, initial squeezing and periodic squeezing to give the same initial rate of entanglement increase, as well as asymptotic entanglement entropy, since no stable islands are present to dampen the entanglement within a full chaotic phase space. This expectation is indeed panned out in our simulations for the three cases where we not only observe the entanglement dynamics of the kicked tops to evolve at the same rate and with the same asymptotic entanglement entropy, they have also converged towards the maximum entanglement entropy of 4.58 for the system, as shown in Figure 11.

We next investigate the effect of j on the quantum-classical correspondence for the kicked-top systems (see Figure 12). We observe that at the deep quantum regime where $j = 5$, the entanglement dynamics is highly fluctuating with both initial and periodic squeezing, consistently giving higher entanglement entropy relative to that of no squeezing. As the system approaches the semi-classical regime at $j = 40$, the entanglement dynamics due to no squeezing becomes comparable to initial squeezing, while periodic squeezing is found to surpass these two cases. At the semi-classical regime of $j = 80$ or $j = 100$, we observe consistent results as those of $j = 80$ discussed earlier. Note that we did not increase j beyond 100 due to computational memory limitations.

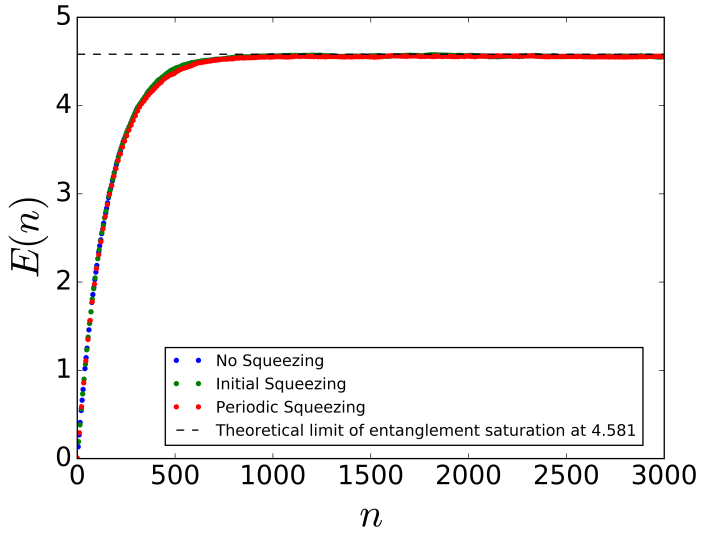

Figure 11. A comparison of the entanglement dynamics for the three cases of no squeezing, periodic spin squeezing and initial spin squeezing, when the kicked tops are in the full chaotic regime at $k = 7.2$. The entanglement rate and asymptotic entanglement entropy for the three cases are found to match closely with each other and converge to the statistical bound of 4.58 in the asymptotic limit. The points are plotted sporadically in order to better show the two curves. The squeezing parameter is set to be $\mu = 0.2$, and the initial state chosen is $\phi = 0.63$ and $\theta = 0.89$.

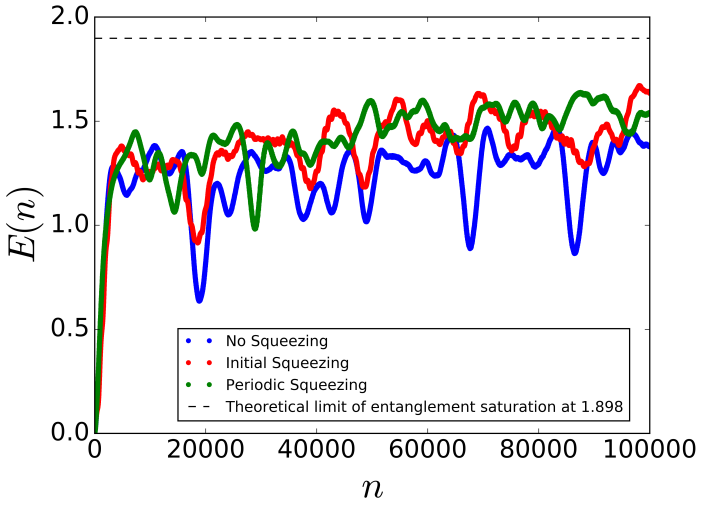

(**a**)

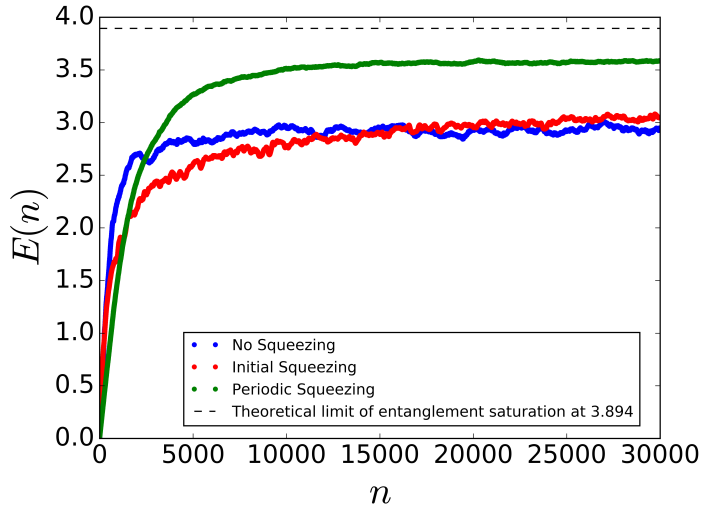

(**b**)

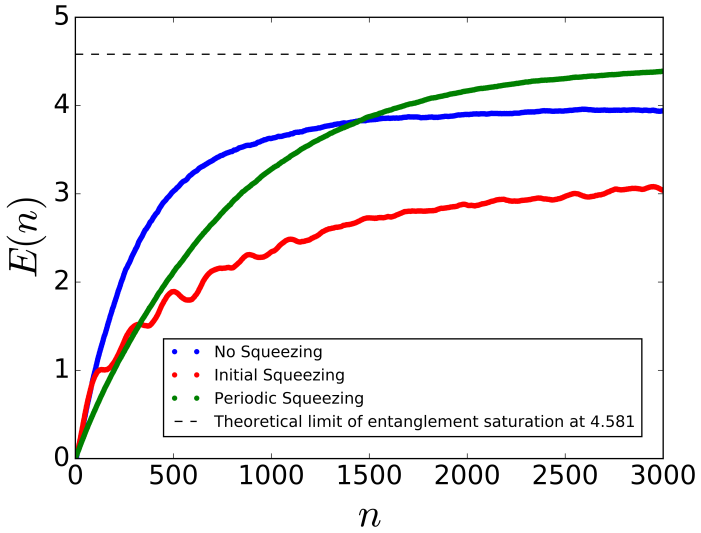

(**c**)

Figure 12. *Cont.*

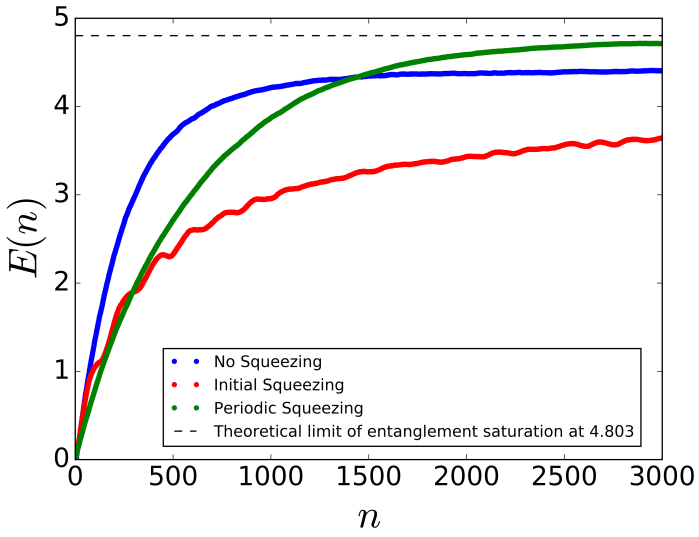

(**d**)

Figure 12. A comparison of the entanglement dynamics for systems of different j. The squeezing parameter is $\mu = 0.2$ and t he initial state chosen here is $\phi = 0.63$ and $\theta = 0.89$. Note that the blue line represents no squeezing, the red line initial squeezing and the green line periodic squeezing. (**a**) $j = 5$; (**b**) $j = 40$; (**c**) $j = 80$; (**d**) $j = 100$.

Finally, we employ the method of quantum power density spectrum [15,39,40] to further analyze the effects of squeezing on the entanglement dynamics of the kicked tops. Note that the quantum power density spectrum is computed by first determining the inner product of the quantum state $|\psi(t)\rangle$ at time t with the quantum state $|\psi(0)\rangle$ at the initial time $t = 0$; after which, Fourier transform is performed on the results to obtain the quantum power density spectrum ρ_{nn} against the energy components E_n.

For the case of no squeezing, we observe that ρ_{nn} has few components for the regular state, but a large number of components for the chaotic state (see Figure 13a,b). This is to be expected, since the number of significant components of ρ_{nn} is directly related to the degree of entanglement of the system. By squeezing the initial regular state, the number of significant components of ρ_{nn} increases (compare Figure 13a,c), while squeezing the chaotic initial state reduces the ρ_{nn} components (compare Figure 13b,d). This supports our earlier claim that initial squeezing of the regular state enhances entanglement, while the same operation on the chaotic state suppresses entanglement. As for periodic squeezing, the much larger number of components of ρ_{nn} for both the regular and chaotic state (see Figure 13e,f) predicts a larger entanglement entropy, which is indeed observed in our earlier simulation results.

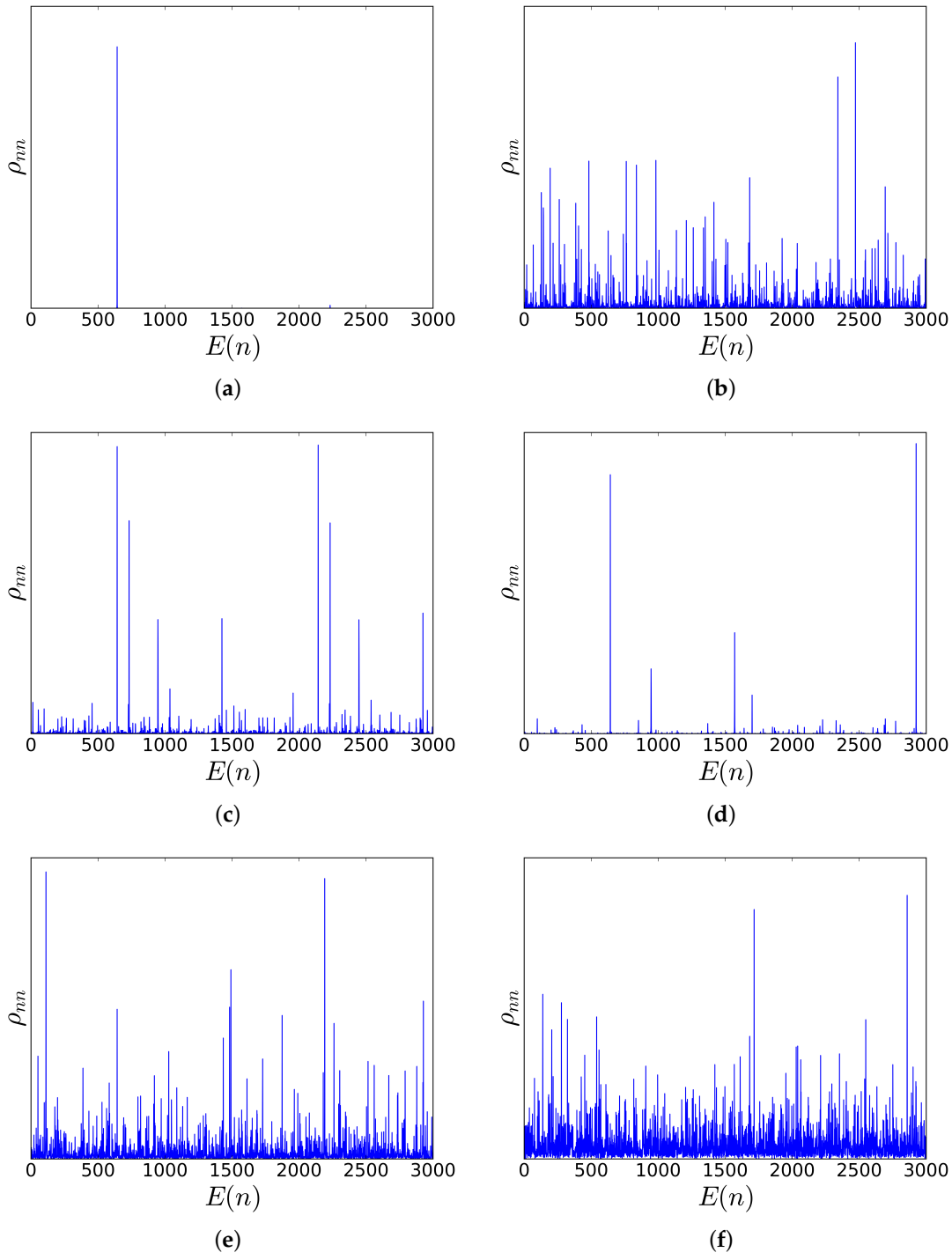

Figure 13. The quantum power density spectrum of the regular initial state ($\theta = 2.25$, $\phi = 0.63$) and the chaotic initial state ($\theta = 0.89$, $\phi = 0.63$) with no squeezing, with initial squeezing and with periodic squeezing. (**a**) Regular state with no squeezing; (**b**) chaotic state with no squeezing; (**c**) regular state with initial squeezing; (**d**) chaotic state with initial squeezing; (**e**) regular state with periodic squeezing; (**f**) chaotic state with periodic squeezing. The act of squeezing is observed to cause the quantum power density spectrum of the regular state in (**c**,**e**) to approach the spectrum for a chaotic state. In (**d**), initial squeezing of a chaotic state leads to a spectrum that corresponds to that which arises from a more regular state, a result that is also observed with respect to the entanglement dynamics.

6. Conclusions

In summary, we have investigated the effects of spin squeezing on two-coupled quantum kicked top systems. Our studies have allowed us to probe into the interesting interface in physics between the classical and quantum domain with respect to chaos and entanglement, respectively. While chaos is purely a classical dynamical behavior and entanglement a solely quantum mechanical effect, our investigations have demonstrated that these two physical entities are intimately connected in the semi-classical regime. In particular, we have shown that the effects of spin squeezing have an important impact on the entanglement between the two quantum kicked tops operating within a classical mixed phase space based on the notion of quantum-classical correspondence. We found that the rate of entanglement is enhanced through initial spin squeezing if the classical analogue of the kicked tops' initial quantum state resides in the regular domain and a slight drop if it resides in the chaotic domain. In addition, our idea of periodic spin squeezing is found to drive the system to attain maximum saturating entanglement entropy quicker than the case of no spin squeezing and initial spin squeezing. Further analysis based on the quantum power density spectrum also yields the same behavior as that of entanglement dynamics, where we observe periodic squeezing to contribute to the largest increase in spectral components, while initial squeezing enhances or suppresses the number of spectral components depending on whether the initial state is regular or chaotic. Our approach thus provides a means to enhance the entanglement of a quantum $\mathcal{N}$ qubits system through exploiting the underlying dynamical behavior of an equivalent set of kicked tops in the classical domain.

There are two aspects of this work that we will leave for future studies. The first relates to the observation of oscillatory behavior in the entanglement dynamics for the cases of initial squeezing (refer to Figure 10a–f) and no squeezing, where the latter is only applicable for initial states lying at the edge between the regular and chaotic region of phase space (see Figure 10b–e). We surmise that this phenomenon arises from the intermittent sampling of the quantum states on the regular and chaotic region of the corresponding classical phase space. The affirmation of this explanation would require further analytical and numerical work. The second aspect concerns possible experimental realization on the theoretical ideas explored in this paper. It is interesting that a quantum kicked top has been experimentally achieved by Chaudhury *et al.* [3] by trapping and laser cooling an ensemble of ^{133}Cs atoms. The atom can be prepared in the spin-coherent state by means of magnetic field pulses, while the twisting is induced through the AC Stark shift in a laser tuned field. Spin squeezing could be achieved by probing the light that interacts with the atoms in the optical cavity. The major challenge would be to isolate two cesium atoms and to induce them to interact with each other (perhaps within a trapping potential), such that we can elucidate their entanglement dynamics and perform quantum-classical correspondence with spin squeezing. Such an experimental design is beyond the scope of this paper and will be pursued in our future studies.

Acknowledgments: The authors would like to thank Wei Shun Lim, Sean Hong Da Ang and Eugene Yong Kang Tay for their invaluable insights and discussions.

Author Contributions: Lock Yue Chew and Ernest Teng Siang Ong conceived of the problem. Ernest Teng Siang Ong performed the simulation and analyzed the data. Both authors wrote the manuscript. Both authors have read and approved the final manuscript.

Conflicts of Interest: The authors declare no conflict of interest.

References

1. Haake, F.; Shepelyansky, D. The kicked rotator as a limit of the kicked top. *Europhys. Lett.* **1988**, *5*, 671–676.
2. Schack, R.; D'Ariano, G.M.; Caves, C.M. Hypersensitivity to perturbation in the quantum kicked top. *Phys. Rev. E* **1994**, *50*, 972–987.
3. Chaudhury, S.; Smith, A.; Anderson, B.E.; Ghose, S.; Jessen, P.S. Quantum signatures of chaos in a kicked top. *Nature* **2009**, *461*, 768–771.
4. Ghose, S.; Stock, R.; Jessen, P.; Lal, R.; Silberfarb, A. Chaos, entanglement, and decoherence in the quantum kicked top. *Phys. Rev. A* **2008**, *78*, 042318.

5. Berry, M.V. The Bakerian lecture, 1987: Quantum chaology. *Proc. R. Soc. Lond. A* **1987**, *413*, 183–198.
6. Berry, M. Quantum chaology, not quantum chaos. *Physica Scripta* **1989**, *40*, 335–336.
7. Haake, F. *Quantum Signatures of Chaos*; Springer: Berlin/Heidelberg, Germany, 2010.
8. Peres, A. Stability of quantum motion in chaotic and regular systems. *Phys. Rev. A* **1984**, *30*, 1610–1615.
9. Emerson, J.; Weinstein, Y.S.; Lloyd, S.; Cory, D. Fidelity decay as an efficient indicator of quantum chaos. *Phys. Rev. Lett.* **2002**, *89*, 284102.
10. Heller, E.J. Bound-state eigenfunctions of classically chaotic Hamiltonian systems: Scars of periodic orbits. *Phys. Rev. Lett.* **1984**, *53*, 1515–1518.
11. Wang, X.; Ghose, S.; Sanders, B.C.; Hu, B. Entanglement as a signature of quantum chaos. *Phys. Rev. E* **2004**, *70*, 016217.
12. Miller, P.A.; Sarkar, S. Signatures of chaos in the entanglement of two coupled quantum kicked tops. *Phys. Rev. E* **1999**, *60*, 1542–1550.
13. Er, C.; Chung, N.N.; Chew, L.Y. Threshold effect and entanglement enhancement through local squeezing of initial separable states in continuous-variable systems. *Physica Scripta* **2013**, *87*, 025001.
14. Joseph, S.K.; Chew, L.Y.; Sanjuan, M.A.F. Effect of squeezing and Planck constant dependence in short time semiclassical entanglement. *Eur. Phys. J. D* **2014**, *68*, 1–11, doi:10.1140/epjd/e2014-50294-0.
15. Joseph, S.K.; Chew, L.Y.; Sanjuán, M.A. Impact of quantum–classical correspondence on entanglement enhancement by single-mode squeezing. *Phys. Lett. A* **2014**, *378*, 2603–2610.
16. Demkowicz-Dobrzański, R.; Kuś, M. Global entangling properties of the coupled kicked tops. *Phys. Rev. E* **2004**, *70*, 066216.
17. Bandyopadhyay, J.N.; Lakshminarayan, A. Entanglement production in coupled chaotic systems: Case of the kicked tops. *Phys. Rev. E* **2004**, *69*, 016201.
18. Steane, A. Quantum computing. *Rep. Prog. Phys.* **1998**, *61*, 117, doi:10.1088/0034-4885/61/2/002.
19. Bouwmeester, D.; Pan, J.W.; Mattle, K.; Eibl, M.; Weinfurter, H.; Zeilinger, A. Experimental quantum teleportation. *Nature* **1997**, *390*, 575–579.
20. Wineland, D.J.; Bollinger, J.J.; Itano, W.M.; Moore, F.L.; Heinzen, D.J. Spin squeezing and reduced quantum noise in spectroscopy. *Phys. Rev. A* **1992**, *46*, R6797–R6800.
21. Leroux, I.D.; Schleier-Smith, M.H.; Vuletić, V. Orientation-dependent entanglement lifetime in a squeezed atomic clock. *Phys. Rev. Lett.* **2010**, *104*, 250801.
22. Louchet-Chauvet, A.; Appel, J.; Renema, J.J.; Oblak, D.; Kjaergaard, N.; Polzik, E.S. Entanglement-assisted atomic clock beyond the projection noise limit. *New J. Phys.* **2010**, *12*, 065032.
23. André, A.; Sørensen, A.S.; Lukin, M.D. Stability of atomic clocks based on entangled atoms. *Phys. Rev. Lett.* **2004**, *92*, 230801.
24. Goda, K.; Miyakawa, O.; Mikhailov, E.E.; Saraf, S.; Adhikari, R.; McKenzie, K.; Ward, R.; Vass, S.; Weinstein, A.J.; Mavalvala, N. A quantum-enhanced prototype gravitational-wave detector. *Nat. Phys.* **2008**, *4*, 472–476.
25. Gühne, O.; Tóth, G. Entanglement detection. *Phys. Rep.* **2009**, *474*, 1–75, doi:10.1016/j.physrep.2009.02.004.
26. Tóth, G.; Knapp, C.; Gühne, O.; Briegel, H.J. Spin squeezing and entanglement. *Phys. Rev. A* **2009**, *79*, 042334.
27. Kitagawa, M.; Ueda, M. Squeezed spin states. *Phys. Rev. A* **1993**, *47*, 5138–5143.
28. Haake, F.; Kuś, M.; Scharf, R. Classical and quantum chaos for a kicked top. *Zeitschrift für Physik B Condensed Matter* **1987**, *65*, 381–395.
29. D'Ariano, G.; Evangelista, L.; Saraceno, M. Classical and quantum structures in the kicked-top model. *Phys. Rev. A* **1992**, *45*, 3646–3658.
30. Glauber, R.J.; Haake, F. Superradiant pulses and directed angular momentum states. *Phys. Rev. A* **1976**, *13*, 357–366.
31. Tinkham, M. *Group Theory and Quantum Mechanics*; Dover Publications: Mineola, NY, USA, 2003.
32. Wigner, E.P. *Group Theory and Its Application to the Quantum Mechanics of Atomic Spectra*; Elsevier: Philadelphia, PA, USA, 2012.
33. Wodkiewicz, K.; Eberly, J.H. Coherent states, squeezed fluctuations, and the $SU(2)$ am $SU(1, 1)$ groups in quantum-optics applications. *J. Opt. Soc. Am. B* **1985**, *2*, 458–466.
34. Johansson, J.R.; Nation, P.D.; Nori, F. QuTiP 2: A Python framework for the dynamics of open quantum systems. *Comput. Phys. Commun.* **2013**, *184*, 1234–1240.

35. Johansson, J.R.; Nation, P.D.; Nori, F. QuTiP: An open-source Python framework for the dynamics of open quantum systems. *Comput. Phys. Commun.* **2012**, *183*, 1760–1772.
36. Wang, X.; Zanardi, P. Quantum entanglement and Bell inequalities in Heisenberg spin chains. *Phys. Lett. A* **2002**, *301*, 1–6, doi: 10.1016/s0375-9601(02)00885-x.
37. Bandyopadhyay, J.N.; Lakshminarayan, A. Testing statistical bounds on entanglement using quantum chaos. *Phys. Rev. Lett.* **2002**, *89*, 060402.
38. Song, L.; Wang, X.; Yan, D.; Zong, Z. Spin squeezing properties in the quantum kicked top model. *J. Phys. B* **2006**, *39*, 559–568.
39. Ghose, S.; Sanders, B.C. Entanglement dynamics in chaotic systems. *Phys. Rev. A* **2004**, *70*, 062315.
40. Zhang, S.-H.; Jie, Q.-L. Quantum-classical correspondence in entanglement production: Entropy and classical tori. *Phys. Rev. A* **2008**, *77*, 012312.